

Dalton Transactions

Accepted Manuscript



This is an *Accepted Manuscript*, which has been through the Royal Society of Chemistry peer review process and has been accepted for publication.

Accepted Manuscripts are published online shortly after acceptance, before technical editing, formatting and proof reading. Using this free service, authors can make their results available to the community, in citable form, before we publish the edited article. We will replace this *Accepted Manuscript* with the edited and formatted *Advance Article* as soon as it is available.

You can find more information about *Accepted Manuscripts* in the [Information for Authors](#).

Please note that technical editing may introduce minor changes to the text and/or graphics, which may alter content. The journal's standard [Terms & Conditions](#) and the [Ethical guidelines](#) still apply. In no event shall the Royal Society of Chemistry be held responsible for any errors or omissions in this *Accepted Manuscript* or any consequences arising from the use of any information it contains.

ARTICLE

New $\text{LaCo}_{0.71(1)}\text{V}_{0.29(1)}\text{O}_{2.97(3)}$ perovskite containing vanadium in octahedral site: synthesis, structural and magnetic characterization.

Cite this: DOI: 10.1039/x0xx00000x

Received 00th January 2012,
Accepted 00th January 2012

DOI: 10.1039/x0xx00000x

www.rsc.org/

V.C. Fuertes^a, M.C. Blanco^a, D.G. Franco^b, S. Ceppi^c, R.D. Sánchez^b, M.T. Fernández-Díaz^d, G. Tirao^c and R.E. Carbonio^{a*}.

In the course of an investigation to prepare the hypothetical new double perovskite $\text{La}_3\text{Co}_2\text{VO}_9$ with Co^{2+} and V^{5+} in octahedral sites we obtain the new simple perovskite $\text{LaCo}_{0.71(1)}\text{V}_{0.29(1)}\text{O}_{2.97(3)}$ as the main phase. The pure compound has then been synthesized by the citrate decomposition method. The crystal structure has been studied by X-ray (PXRD) and neutron powder diffraction (PND). Physical properties were characterized by X-ray absorption spectroscopy (XAS), X-ray emission spectroscopy (XES) and thermogravimetric measurements (TGA). Rietveld refinements were performed in the orthorhombic space group Pnma (#62). Refined cell parameters were $a = 5.4762(2)$ Å, $b = 7.7609(2)$ Å and $c = 5.5122(1)$ Å. Magnetization measurements showed that this perovskite is an antiferromagnet with Neel temperature of 15 K. At high T the magnetization follows the Curie-Weiss law corrected by temperature independent paramagnetism (TIP) showing an effective magnetic moment of $3.03 \mu_B$ well described by the contribution of Co^{2+} (HS), Co^{3+} (IS), V^{3+} and V^{4+} ions. The crystallographic formula was refined by PND and oxidation states distribution was determined by the combination of PND, XAS, TGA and magnetic measurements.

Introduction

Perovskite compounds are very interesting materials because they show a wide variety of physical phenomena such as catalysis [1], electronic and ionic transport [2], multiferroism [3], among others. In this context, the perovskite structure ABO_3 represents an attractive system due to its easy-to-control physical properties derived from the diverse range of ions and oxidation states which can be incorporated into the structure. It can accommodate almost all elements of the periodic table on its cuboctahedral (A) and octahedral (B) sites. The relative size of the A and B cations can drive several distortions being the main one the tilting of the octahedra [4]. Moreover, solid solutions may be formed by replacing two different transition cations in crystallographic octahedral B-sites and they can be either ordered or disordered within the structure.

The B site can be occupied by a wide variety of representative, transition and rare earth elements. In several reports the Co containing perovskite oxides exhibit a coexistence of Co^{2+} and Co^{3+}

ions on B-sites [5]. Presences of such mixed electronic states allow different magnetic interactions which contribute to the magnetic behavior. Moreover, the Co^{3+} ions have spin state variability where the d electrons can show: high-spin (HS) $t_{2g}^4 e_g^2$, intermediate spin (IS) $t_{2g}^5 e_g^1$ or low-spin (LS) t_{2g}^6 states, although LS is not observed in oxides since O^{2-} ion is a weak ligand. On the other hand, Co^{2+} (HS) ion frequently shows unquenched orbital contribution in a quasi-regular octahedral environment [6, 7], even though many times, this ion and the rest of the transition metal ions of the first series have spin only contribution.

Instead of the diamagnetic V^{5+} (d^0) ion which rarely occupy octahedral sites because of its very low size for such sites, the paramagnetic V^{3+} (d^2) and V^{4+} (d^1) ions can occupy the octahedral sites and contribute to the many magnetic interactions. An example of this is the disordered perovskite La_2CoVO_6 , which was reported by Holman et al. as belonging to the orthorhombic space group Pnma, where the oxidation states of Co and V ions are $2+$ and $4+$ respectively [8]. Other simple perovskite with Pnma orthorhombic

symmetry is $\text{LnMn}_3\text{V}_4\text{O}_{12}$ (Ln= La, Nd, Gd, Y, Lu) synthesized under high-pressure conditions by Shimakawa et al. [9], where the vanadium has the oxidation state 3.75+. Also mixed oxidation states for vanadium in perovskite octahedral sites were reported for La_2MnVO_6 double perovskite [10].

Mixed valence systems are very interesting from many points of view. It is well known that Kobayashi et al. [11] reported room temperature magnetoresistance in $\text{Sr}_2\text{FeMoO}_6$ in which ferromagnetic and half metallic behavior is due to the mixed valences of Fe and Mo ions.

Mixed valence systems provide a unique opportunity to investigate the contribution of solid state chemistry to electrocatalytic activity [12]. Numerous studies may be mentioned on the use of mixed valence compounds as electrodes in solid oxide fuel cells [13-15]. In fact, the study of the electronic and magnetic properties of Co-based perovskites has been intimately connected to the existence of spin-state transitions and with the study of the presence of oxygen vacancies, necessary for oxide ions migration through cathodes and anodes [16, 17].

Few reports are about perovskite oxides with $d^1 \text{V}^{4+}$ ions in octahedral sites [18] and even less, those that combine Co and V ions [8]. To the best of our knowledge, this is the first work that presents a combination of d^7 (HS) Co^{2+} , d^6 (IS) Co^{3+} , V^{3+} and V^{4+} ions in perovskite octahedral sites. Moreover if the material can present oxygen vacancies, all these characteristics make this material very interesting from a technological point of view (catalysis, SOFC, ionic conductors, etc.). In the present article we describe the synthesis, structural and magnetic characterization of the new simple perovskite $\text{LaCo}_{0.71(1)}\text{V}_{0.29(1)}\text{O}_{2.97(3)}$. We have used powder X-ray diffraction (PXRD) and powder neutron diffraction (PND), magnetization vs. temperature measurements, Co ion oxidation state determination from X-ray absorption spectroscopy (XAS), $\text{K}\beta$ X-ray Emission Spectroscopy (XES) and thermogravimetric analysis (TGA).

Materials and methods

A powdered sample of the perovskite $\text{LaCo}_{0.71(1)}\text{V}_{0.29(1)}\text{O}_{2.97(3)}$ was prepared by citrate decomposition method. Stoichiometric amounts of $\text{La}(\text{NO}_3)_3 \cdot 6\text{H}_2\text{O}$, $\text{Co}(\text{NO}_3)_2 \cdot 6\text{H}_2\text{O}$ and NH_4VO_3 , in analytic grade, were dissolved in a solution of citric acid 30% W/V, maintaining a concentration ratio of citric acid/total metal concentration= 1. Small amounts of HNO_3 (65% W/V) were added to facilitate reagents dissolution.

The reaction mixture was heated under stirring until the formation of a dark brown gel. This powder precursor was then dried for 24 h at 100 °C and subsequently heated up to 300 °C for 3 h and up to 600 °C for 20 h in air atmosphere to remove water and residual organic compounds. Finally, the product was pressed into a pellet and heat treated in a platinum crucible at 1400 °C for a period of 10 h under Ar atmosphere.

The high phase purity (98.4 %, with CoO as minority phase) was confirmed by PXRD data measured on a PANalytical X'Pert PRO powder diffractometer (40kV, 40mA), in Bragg-Brentano reflection geometry with $\text{CuK}\alpha$ radiation ($\lambda = 1.5418 \text{ \AA}$). The data were obtained between 5° and 120° in 2θ in steps of 0.02° and counting time of 6 seconds per step. The PND pattern was collected at RT in the D1A diffractometer at Institute Laue-Langevin (ILL), Grenoble, France. The wavelength was 1.910 Å and the 2θ range was from 0° to 160°, with increments of 0.05°. The coherent scattering lengths for La, V, Co and O are 0.824, -0.0382, 0.2490 and 0.5803 fm

respectively. Despite the very low scattering length of V, since we will be refining the position and occupation of a site which is occupied simultaneously by Co and V, the large difference between the neutrons scattering lengths of both elements will allow us to refine the occupancies with confidence.

The refinement of the crystal structure was performed by the Rietveld method [19] using the FULLPROF program [20]. A pseudo-Voigt shape function was adequate to obtain good fits. The polyhedral perspective of the crystal structure was plotted using the program Vesta (version 3.1.8) [21].

XAS and $\text{K}\beta$ X-ray emission spectroscopy (XES) [22] have been used for the determination of the oxidation states of Co ions. High-resolution $\text{K}\beta$ XES and K edge XAS spectra of $\text{LaCo}_{0.71(1)}\text{V}_{0.29(1)}\text{O}_{2.97(3)}$ perovskite and two cobalt compounds with known Co oxidation states ($\text{BiLa}_2\text{Co}_2\text{SbO}_9$ and LaCoO_3) were measured at the D12A-XRD1 beamline of the "Laboratorio Nacional de Luz Sincrotrón" (LNLS, Campinas, Brazil), using a non-conventional spectrometer, based on quasi-back diffraction geometry [22], from which it is possible to determine the Co chemical environment by examining spectral features of the measured spectra. The Co- $\text{K}\beta$ XES spectra were normalized to the incident intensity to consider beam fluctuations. To calculate the spectral parameters, the spectra were then normalized to a constant value for the maximum and a linear background was subtracted. Two Voigt functions, representing the $\text{K}\beta'$ and $\text{K}\beta_{1,3}$ peaks, and a EMG (Exponentially Modified Gaussian) function, representing the radiative Auger effects (RAE) and $\text{K}\beta_x$ line, were fitted in order to reproduce the peaks features [23]. With a spot size of 1.2 mm², the measured counting rate at the main peak ($\text{K}\beta_{1,3}$ line) was around 200 and the signal to background ratio was better than 100. The resolution of this spectrometer was determined to be 3.1 eV for the $\text{K}\beta_{1,3}$ line. For calculation details see Ref. 22. The experimental errors of the studied spectral parameters were determined from the fitting errors. The XAS spectra were collected in the fluorescence mode using the same experimental setup for XES. The analyser was positioned in the maximum of the fluorescence spectra ($\text{K}\beta_{1,3}$ line) and the spectra were measured only in the X-ray absorption near edge structure (XANES) region using the Si(111) beam line monochromator. The spectra were normalized to the edge jump and the edge position was determined by the maximum of the first derivative [24].

The magnetic measurements were performed in a commercial Quantum Design MPMS-5S superconducting quantum interference device (SQUID) magnetometer on powdered samples, in the 5–300 K temperature range and magnetic fields up to 5 T.

Thermogravimetric measurements were carried out in a Shimadzu DTG-60 Thermoanalyzer, in the 30–980 °C temperature range under an oxidizing atmosphere (air) in order to evaluate the oxidation states of cobalt and vanadium ions.

Results

In the course of an investigation to prepare the hypothetical new double perovskite $\text{La}_3\text{Co}_2\text{VO}_9$ with Co^{2+} and V^{5+} in octahedral sites, samples prepared by the sol gel method between 1000 and 1400 °C during 10 h in an Ar inert atmosphere were obtained. PXRD and PND patterns for each sample did not show single phase of the expected double perovskite (see Figures S1 and S2 in the Supplementary Information). PND data analysis for the sample allowed us to refine occupancies on all the sites of the simple perovskite phase structure and determine its real composition. From these results, we observed that the real stoichiometry was

$\text{LaCo}_{0.73}\text{V}_{0.27}\text{O}_3$ showing the possibility that a fraction of Co^{2+} be oxidized to Co^{3+} (due to instability of Co^{2+}). This simple perovskite was mixed with minority phases LaCoO_3 , V_2O_5 and La_2O_3 .

Subsequently, a new synthesis was undertaken to confirm the last proposed composition. Now, appropriate amounts of reactants were used to prepare the sol-gel precursor and fired at 1400 °C in an Ar inert atmosphere for 10 hours.

The PXRD and PND results were refined by Rietveld analysis and showed a good agreement with an orthorhombic cell (space group Pnma) corresponding to a simple perovskite model.

Structural characterization

Figures 1 and 2 show PXRD and PND data at RT for $\text{LaCo}_{0.71(1)}\text{V}_{0.29(1)}\text{O}_{2.97(3)}$ as a main phase (>98%), CoO is the minority phase. Analyses of these data indicate that this phase crystallizes in the orthorhombic Pnma space group. This space group is described by the $a^-b^+a^-$ tilt system of two octahedral tilts in the Glazer notation [25, 26], see Figure 3.

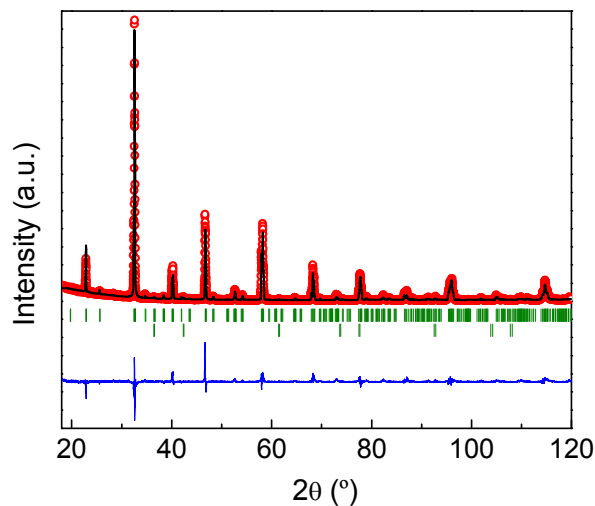


Figure 1: Rietveld refinement of the PXRD pattern at room temperature for a sample with stoichiometry $\text{LaCo}_{0.71(1)}\text{V}_{0.29(1)}\text{O}_{2.97(3)}$. Vertical marks correspond to the position of the allowed Bragg reflections. Upper marks: $\text{LaCo}_{0.71(1)}\text{V}_{0.29(1)}\text{O}_{2.97(3)}$ (98.4(1)%); Lower marks: CoO (1.6(1)%).

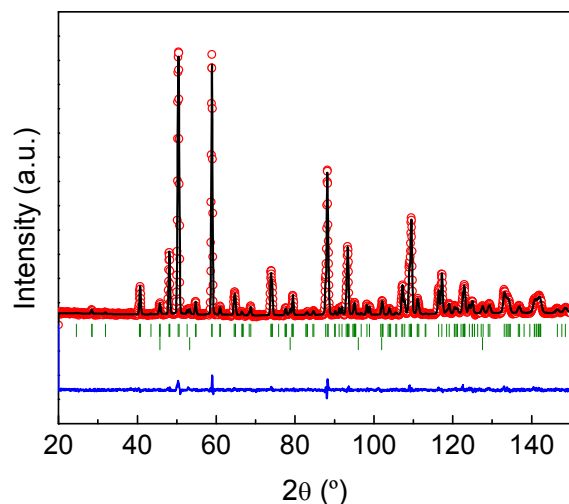


Figure 2: Rietveld refinement of the PND pattern at room temperature for a sample with stoichiometry $\text{LaCo}_{0.71(1)}\text{V}_{0.29(1)}\text{O}_{2.97(3)}$ (S.G.: Pnma). Minority phase corresponds to CoO.

Table 1 shows refined atomic positions for this new perovskite, while selected bond lengths and bond angles at RT are given in Table 2. The different (Co/V)-O bond lengths are very similar leading to quite regular octahedra. The BO_6 octahedral tilt angles can be defined as $\delta = (180 - \theta)/2$, where θ is a (Co/V)-O-(Co/V) angle. The tilt is consistent with the space group Pnma (#62) and with the Goldschmidt tolerance factor which falls slightly below unity, $\tau = 0.96$. τ was calculated using the well known formula: $\tau = (R_A + R_O) / \sqrt{2(\langle R_B \rangle + R_O)}$, where R_A is the La^{3+} radius for XII coordination (1.5 Å), R_O is the O^{2-} radius for VI coordination (1.26 Å) and $\langle R_B \rangle$ is the average ionic radius of the cations occupying the B site in VI coordination, according to the formula: $\langle R_B \rangle = 0.21 r\text{Co}^{2+} + 0.50 r\text{Co}^{3+} + 0.14 r\text{V}^{3+} + 0.15 r\text{V}^{4+}$. The values of radii of all the transition cations were taken for HS, since value for IS Co^{3+} was not available ($r\text{Co}^{2+} = 0.885$ Å; $r\text{Co}^{3+} = 0.75$ Å; $r\text{V}^{3+} = 0.78$ Å and $r\text{V}^{4+} = 0.72$ Å).

Atom	x	y	z	Occ	B_{iso}
La (4c)	0.0215(1)	0.25000	0.9957(1)	1.00	0.84(2)
V (4b)	0.5000	0.0000	0.0000	0.29(1)	0.19(6)
Co (4b)	0.5000	0.0000	0.0000	0.71(1)	0.19(6)
O1 (4c)	0.4940(2)	0.2500	0.0651(2)	0.97(1)	0.51(4)
O2 (8d)	0.2756(1)	0.03415(8)	0.7251(1)	1.00(1)	0.99(2)

Table 1: Refined atomic positions, occupancies and thermal factors obtained at RT from combined Rietveld refinement of PND and PXRD data for the perovskite $\text{LaCo}_{0.71(1)}\text{V}_{0.29(1)}\text{O}_{2.97(3)}$ (S.G.: Pnma). Refined cell parameters: $a = 5.4762(2)$ Å, $b = 7.7609(2)$ Å and, $c = 5.5122(1)$ Å. Discrepancy factors PND: $R_p = 14.5$, $R_{wp} = 16.7$, $R_{exp} = 9.40$, $\chi^2 = 3.14$. Discrepancy factors PXRD: $R_p = 12.6$, $R_{wp} = 16.9$, $R_{exp} = 6.53$, $\chi^2 = 6.73$.

Distances (Å)	(Co/V)-O1	$2 \times 1.9734(2)$
	(Co/V)-O2	$2 \times 1.9692(6)$
	(Co/V)-O2	$2 \times 1.9714(6)$
	<(Co/V-O)>	1.9713
Angles (degrees)	(Co/V)-O1-(Co/V)	158.952(7)
	(Co/V)-O2-(Co/V)	160.73(3)
Tilt angles (degrees)	δ	10.52
		9.64

Table 2: Selected bond distances and angles and Tilt angles (δ) at RT obtained from Rietveld refinement of PND data (shown in Figure 1) for the perovskite $\text{LaCo}_{0.71(1)}\text{V}_{0.29(1)}\text{O}_{2.97(3)}$.

Combined refinements of PXRD and PND data were performed by allowing the variations of the occupancies of the metal ions in octahedral sites and O^{2-} sites resulting in a small amount of oxygen vacancies. Thus, the refined crystallographic formula can be written as $\text{LaCo}_{0.71(1)}\text{V}_{0.29(1)}\text{O}_{2.97(3)}$.

XAS is a conventional technique to analyse the chemical environment of an element in an unknown material. The edge energy for an element in a higher oxidation state is usually shifted several electron volts to higher X-ray energies [24], see Figure 4. From the linear interpolation of known oxidation states, Co^{2+} in $\text{BiLa}_2\text{Co}_2\text{SbO}_9$ and Co^{3+} in LaCoO_3 , see inset of Figure 4, the average Co oxidation state in $\text{LaCo}_{0.71(1)}\text{V}_{0.29(1)}\text{O}_{2.97(3)}$ was calculated to be 2.7 ± 0.2 . It can be established the final composition for the perovskite as $\text{LaCo}_{0.21}^{2+}\text{Co}_{0.50}^{3+}\text{V}_{0.14}^{3+}\text{V}_{0.15}^{4+}\text{O}_{2.97}$, by the appropriated combination of both the stoichiometric and chemical environment information from PND data and XAS data.

The questions that can be raised are: Why the initially proposed composition was not stable? And, why this specific composition is

the stable one under the present experimental conditions? In principle it can be stated that the original “double perovskite” with Co^{2+} and V^{5+} (i.e. $\text{La}_3\text{Co}_2\text{VO}_9$) is not stable because it is not possible to stabilize the highly oxidized V^{5+} cation in presence of the reduced Co^{2+} cation, which on the other hand, needs the mild reducing condition of the Ar atmosphere. A general chemical equilibrium is then established under the experimental conditions: $\text{V}^{5+} + \text{Co}^{2+} \leftrightarrow x \text{V}^{4+} + y \text{V}^{3+} + z \text{Co}^{3+} + (1-z) \text{Co}^{2+}$, where x , y and z were determined for the present sample. However, there could be an infinite number of other possible compositions, but these compositions are not compatible with the (unknown) O_2 partial pressure in equilibrium with the sample at 1400°C in Ar atmosphere. To reach some of these other compositions it should be necessary to control the partial O_2 pressure at other values and tune the specific composition compatible with the stable oxidation states.

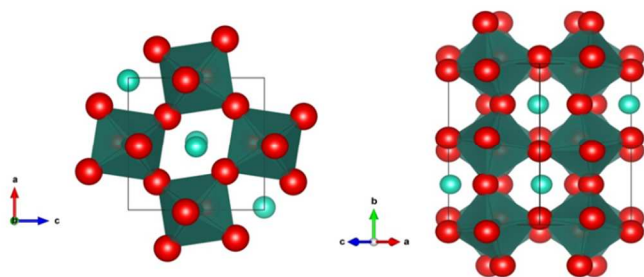


Figure 3: A polyhedral view of the orthorhombic structure of $\text{LaCo}_{0.71(1)}\text{V}_{0.29(1)}\text{O}_{2.97(3)}$ obtained from PXRD and PND data taken at RT showing: *inphase* (+) rotation along the b axis (left) and *antiphase* (-) rotation (right) along the a (or c) of the pseudocubic cell. The octahedra represent $(\text{Co}/\text{V})\text{O}_6$, red (online) spheres represent the oxide ions and light-blue (online) spheres represent the La^{3+} ions.

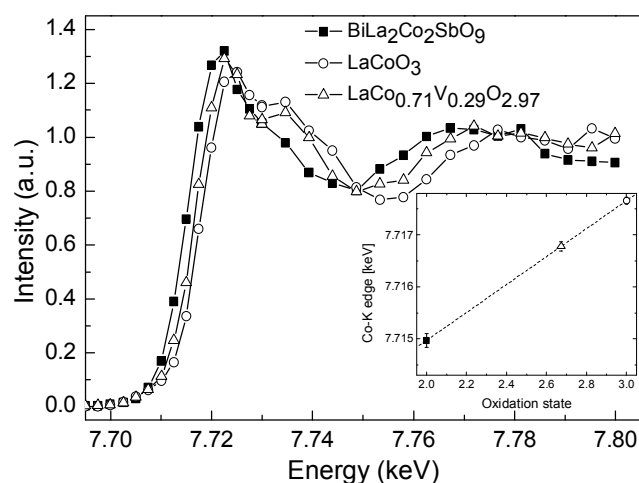
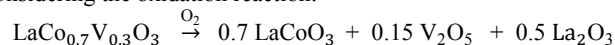


Figure 4: Near edge Cobalt K absorption spectra of $\text{LaCo}_{0.71(1)}\text{V}_{0.29(1)}\text{O}_{2.97(3)}$ and references $\text{BiLa}_2\text{Co}_2\text{SbO}_9$, LaCoO_3 with known Co oxidation state. Inset: Cobalt oxidation state determination by linear interpolation of edge position determined by the maximum of first derivative.

XES has been widely used for elemental analysis and for studying the electronic structure of atoms [27]. In transition metal compounds $\text{K}\beta$ XES spectra resulting from transitions $3p-1s$, consist of the main $\text{K}\beta_{1,3}$ line and satellite structures. The $\text{K}\beta'$ satellite line could be

qualitatively explained using a simple $3p3d$ exchange interaction model proposed by Tsutsumi et al. [28]. This model points that the intensity of the $\text{K}\beta'$ line ($\text{IK}\beta'$) increases with the cation nominal spin. Figure 5 shows the $\text{K}\beta'$ - $\text{K}\beta_{1,3}$ region of the Co-K β spectra for the studied compounds. It can be seen a clear difference of $\text{IK}\beta'$ for the $\text{BiLa}_2\text{Co}_2\text{SbO}_9$ and LaCoO_3 compounds being the $\text{IK}\beta'$ for the first higher than for the second. It is not the case for $\text{LaCo}_{0.71(1)}\text{V}_{0.29(1)}\text{O}_{2.97(3)}$ and LaCoO_3 compounds, where the $\text{IK}\beta'$ are very similar. Therefore the $\text{BiLa}_2\text{Co}_2\text{SbO}_9$ nominal spin is greater than LaCoO_3 and both $\text{LaCo}_{0.71(1)}\text{V}_{0.29(1)}\text{O}_{2.97(3)}$ and LaCoO_3 have spin states which can be considered similar. The spin state of LaCoO_3 is reported as IS ($S=1$) [29] or as a mixture of LS ($S=0$) and HS ($S=2$) states for Co^{3+} ions [30]. Both materials have similar behavior of $\text{IK}\beta'$ lines and can be understood if, in $\text{LaCo}_{0.71(1)}\text{V}_{0.29(1)}\text{O}_{2.97(3)}$ perovskite, the spin state of Co^{2+} ions is HS while that of Co^{3+} ions is IS.

TGA consistently shows that $\text{LaCo}_{0.71(1)}\text{V}_{0.29(1)}\text{O}_{2.97(3)}$ begins to gain weight due to oxidation of Co^{2+} , V^{3+} and V^{4+} . The experimental value of $\sim 1\%$ (see Figure 6) is in agreement with the calculated one considering the oxidation reaction:



In addition, the Rietveld analysis of PXRD pattern for the thermogravimetric solid residue is in good agreement with the proposed products (See Figure S3 in the Supplementary Information), confirming thereby the original distribution of oxidation states of the cations Co^{2+} , Co^{3+} , V^{3+} and V^{4+} . Similar studies were presented by Pascanut et al. [31] for $\text{SrTi}_{1-x}\text{Co}_x\text{O}_3$.

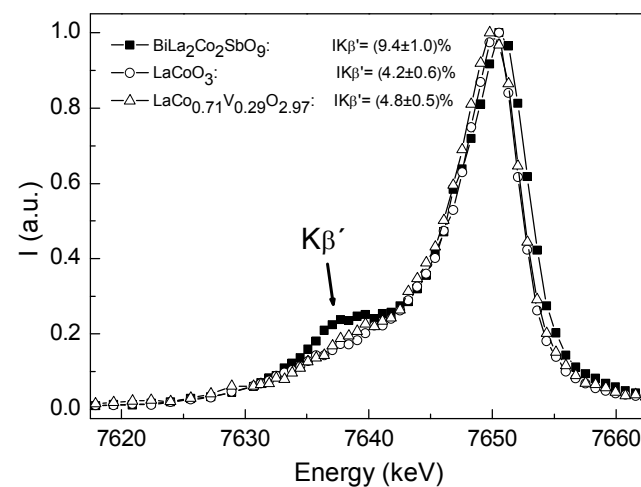


Figure 5: Cobalt $\text{K}\beta$ XES spectra of $\text{LaCo}_{0.71(1)}\text{V}_{0.29(1)}\text{O}_{2.97(3)}$. Comparison with $\text{BiLa}_2\text{Co}_2\text{SbO}_9$ and LaCoO_3 . The intensity of the total area for the $\text{K}\beta'$ ($\text{IK}\beta'$) is included in the top of the figure.

Magnetic characterization

In Figure 7, we show the magnetic susceptibility (χ) taken as M/H measured at $H=5$ kOe. Decreasing temperature, χ increases continuously down to 15 K where it can be observed a change of the regime, suggesting that the material reaches a magnetic ordered state. In this state, the M vs H plot at 5 K shows a linear behavior between -10 kOe and 10 kOe, which is in agreement with a typical response of an antiferromagnetic (AFM) material. χ exhibits a TIP contribution (α), which is more visible at high temperatures. To subtract this TIP value from χ , we adjust magnetic data using a

model with a Curie-Weiss term and an extra TIP contribution to describe the paramagnetism of the system. **Equation 1** was used in the range between 50 and 300 K, where C is the Curie constant, θ is the Curie-Weiss temperature and α the TIP contribution.

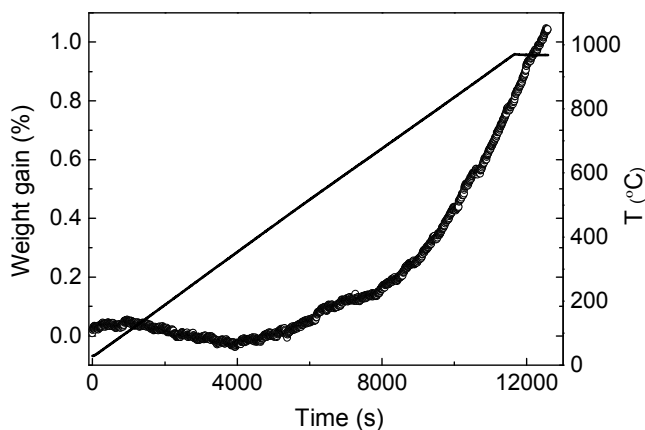


Figure 6: TGA measured in the 30-980 °C temperature range under air atmosphere (75 mL min^{-1}) for the $\text{LaCo}_{0.71(1)}\text{V}_{0.29(1)}\text{O}_{2.97(3)}$ perovskite. The final temperature was maintained during 30 min to complete oxidation.

$$\chi = \frac{c}{(T-\theta)} + \alpha \quad (\text{Eq. 1})$$

The parameters obtained are $\theta = -55.68(1) \text{ K}$, $C = 1.147(5) \text{ emu K/Oe g}$ and $\alpha = (4.02 \pm 0.06) \times 10^{-6} \text{ emu/Oe g}$.

In order to check the Curie Weiss behavior, we subtract α to the susceptibility and plot the reciprocal ($1/(\chi-\alpha)$) as a function of T in the inset of **Figure 7**. A linear behavior can be observed in the temperature range fitted (50-300 K). The negative θ values confirms that antiferromagnetic interactions are present in this perovskite. From the Curie constant we obtain $\mu_{\text{eff}} = 3.03(1) \mu_{\text{B}}$.

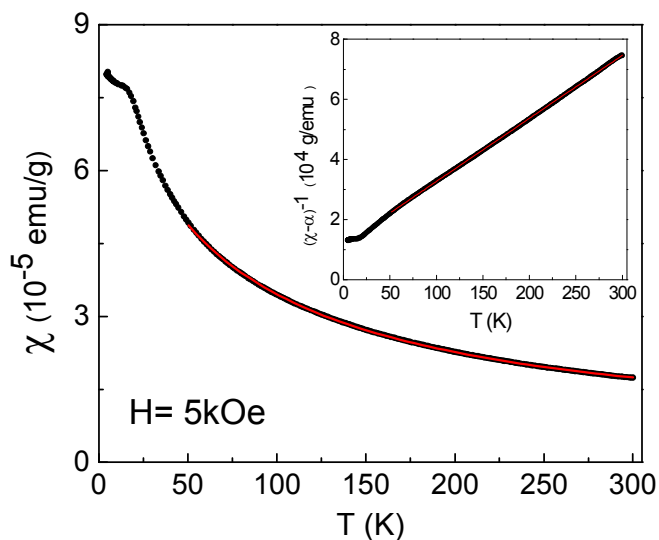


Figure 7: Magnetic susceptibility (χ) versus Temperature (T) in the 5 to 300 K range. The inflection point indicates the Neel temperature

$T_{\text{N}} \cong 15 \text{ K}$. Line (Red online) is the data fit result using a Curie-Weiss law with an extra temperature independent paramagnetic (α) term. Inset shows $(\chi-\alpha)^{-1}$ as a function of T .

Magnetic properties of the Co^{2+} cation are sensible to the environment and generally difficult to describe theoretically. The spin only contribution is $\mu_{\text{eff}} = 3.87 \mu_{\text{B}}$. However, in inorganic complexes and some oxides, an important spin-orbit contribution could be present and higher values are usually observed $\mu_{\text{eff}} = 4.7\text{-}5.2 \mu_{\text{B}}$. The real value should lie between these two limits. For simplicity, we assume in our case spin only contribution. By using the formula $\mu_{\text{eff}}^2 = 0.21(\mu_{\text{Co}^{2+}})^2 + 0.50(\mu_{\text{Co}^{3+}})^2 + 0.14(\mu_{\text{V}^{3+}})^2 + 0.15(\mu_{\text{V}^{4+}})^2$, calculated μ_{eff} for $\text{LaCo}_{0.21}\text{Co}_{0.50}\text{V}_{0.14}\text{V}_{0.15}\text{O}_{2.97}$ perovskite is $2.95 \mu_{\text{B}}$ which is very close to the experimental one ($3.03(1) \mu_{\text{B}}$), which supports our assumption of quenched orbital magnetic moment for Co^{2+} . This picture is also in agreement with XES results. The used individual magnetic moments were $3.87 \mu_{\text{B}}$ (Co^{2+} (HS) spin only), $2.83 \mu_{\text{B}}$ (Co^{3+} (IS)), $2.83 \mu_{\text{B}}$ (V^{3+}) and $1.73 \mu_{\text{B}}$ (V^{4+}).

The presence of these magnetic ions occupying the same crystallographic site in a completely disordered structure lead to various magnetic interactions ($d^1\text{-}d^6$, $d^2\text{-}d^7$, $d^2\text{-}d^2$, $d^7\text{-}d^7$, among others) which on average are expressed by an antiferromagnetic behavior. TIP can be considered to come from the contribution of the t_{2g} electrons in the V^{3+} and V^{4+} cations [32].

Conclusions

The new perovskite with $\text{V}^{3+/4+}$ ions in octahedral sites was successfully synthesized by citrate decomposition. The crystal structure was well characterized by the orthorhombic space group Pnma , with cell parameters $a = 5.4762(2) \text{ \AA}$, $b = 7.7609(2) \text{ \AA}$ and $c = 5.5122(1) \text{ \AA}$. This disordered orthorhombic perovskite has the $a'b^+a^-$ Glazer tilt system, with a very slight distortion of the octahedra.

Through XAS results it could be determined the average oxidation state for cobalt cations as 2.7 ± 0.2 , showing coexistence of Co^{2+} and Co^{3+} ions.

Combination of PND, TGA and XAS data allowed us to determine the real stoichiometry and the oxidation states distribution of the transition metal cations so that the chemical formula can be written: $\text{LaCo}_{0.21}\text{Co}_{0.50}\text{V}_{0.14}\text{V}_{0.15}\text{O}_{2.97}$. In addition, XES results allow us to determine IS behavior for Co^{3+} ion. Thus, this important result about the mixed oxidation states distribution is a contribution for several very important technological applications like catalysis, SOFC's, solid electrolytes, etc.

Magnetization measurements showed that the perovskite is an antiferromagnet with Neel temperature of 15 K. At high T it follows the Curie-Weiss law corrected by TIP and showing an effective magnetic moment of $3.03 \mu_{\text{B}}$ which is in perfect agreement with the magnetic moment calculated with the oxidation states distribution of Co^{2+} (HS), Co^{3+} (IS) and V^{3+} and V^{4+} ions obtained with the other techniques.

Acknowledgements

R.E.C. thanks support from Consejo Nacional de Investigaciones Científicas y Técnicas (CONICET), PIP #11220120100360, the Agencia Nacional de Promoción Científica y Tecnológica (ANPCyT) PICT-2013-2149 and the Secretaria de Ciencia y Tecnología de la Universidad Nacional de Córdoba (SECyT-UNC), Project 203/14. V.C.F. thanks support from the Agencia Nacional de Promoción Científica y Tecnológica (ANPCyT) PICT-2013-0022.

R.D.S. acknowledges support from grants ANPCyT PICT 2011-752, CONICET PIP 0490 and SECyT-UNCuyo 06/C456. We gratefully acknowledge the Institut Laue Langevin (ILL) (Grenoble, France) for access to D2B powder diffractometer.

Notes and references

^a INFIQC-CONICET, Dpto. de Físicoquímica, Fac. de Ciencias Químicas, U.N.C., Córdoba (5000), Argentina.

^b Centro Atómico Bariloche, Comisión Nacional de Energía Atómica and Instituto Balseiro, Universidad Nacional de Cuyo, Bariloche (8400), Río Negro, Argentina.

^c IFEG-CONICET, Fac. de Matemáticas, Astronomía y Física, U.N.C., Córdoba (5000), Argentina.

^d Institut Max Von Laue Paul Langevin, F-38042, Grenoble Cedex 9, France.

*Author to whom correspondence should be addressed. Mailing Address: INFIQC (CONICET). Departamento de Físicoquímica. Facultad de Ciencias Químicas. Universidad Nacional de Córdoba. Haya de la Torre esq. Medina Allende. Ciudad Universitaria. X5000HUA. Córdoba. Argentina. Phone: +54-351-5353866 (ext. 53556), Fax: +54-351-433-4188, E-mail: carbonio@fcq.unc.edu.ar

†Electronic Supplementary Information (ESI) available:

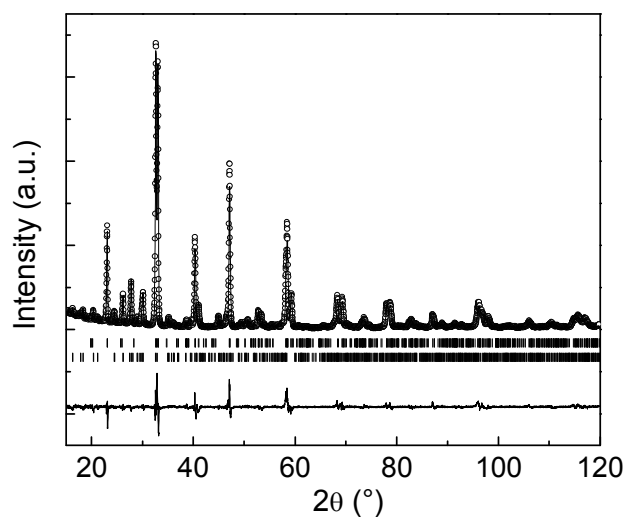


Figure S1: Rietveld refinement of the PXRD pattern at room temperature for a sample with stoichiometry $\text{La}_3\text{Co}_2\text{VO}_9$ synthesized by sol gel method. Main phase: $\text{LaCo}_{0.73}\text{V}_{0.27}\text{O}_3$; impurity phase: LaVO_4 .

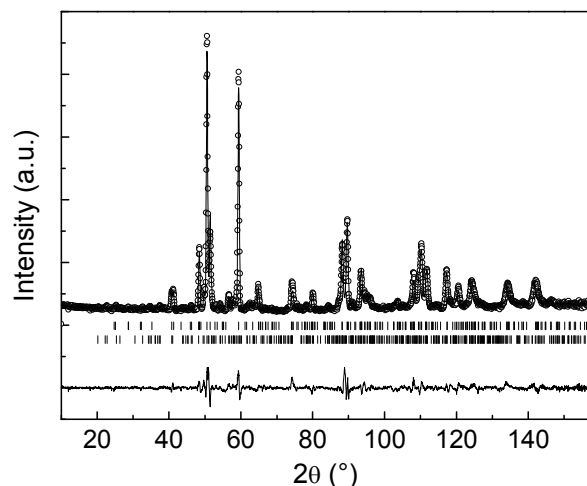


Figure S2: Rietveld refinement of PND pattern at room temperature for a sample with stoichiometry $\text{La}_3\text{Co}_2\text{VO}_9$ synthesized by sol gel method. Main phase: $\text{LaCo}_{0.73}\text{V}_{0.27}\text{O}_3$; impurity phase: LaVO_4 .

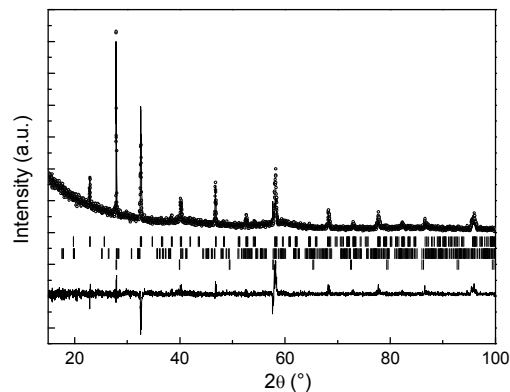


Figure S3: Rietveld analysis of PXRD pattern for the thermogravimetric solid residue. Vertical marks correspond to the position of the allowed Bragg reflections. Upper marks: LaCoO_3 (61.3(2)%); Middle marks: V_2O_5 (13.5(2)%); Lower marks: La_2O_3 (25.2(1)%). Due to the high preferential orientation produced by sample preparation on the zero background sample holder (Silicon single crystal), the percentages are not close to the theoretical ones (47,5% for LaCoO_3 , 7,5% for V_2O_5 and 45% for La_2O_3), but all the reflections can be explained with the proposed compounds.

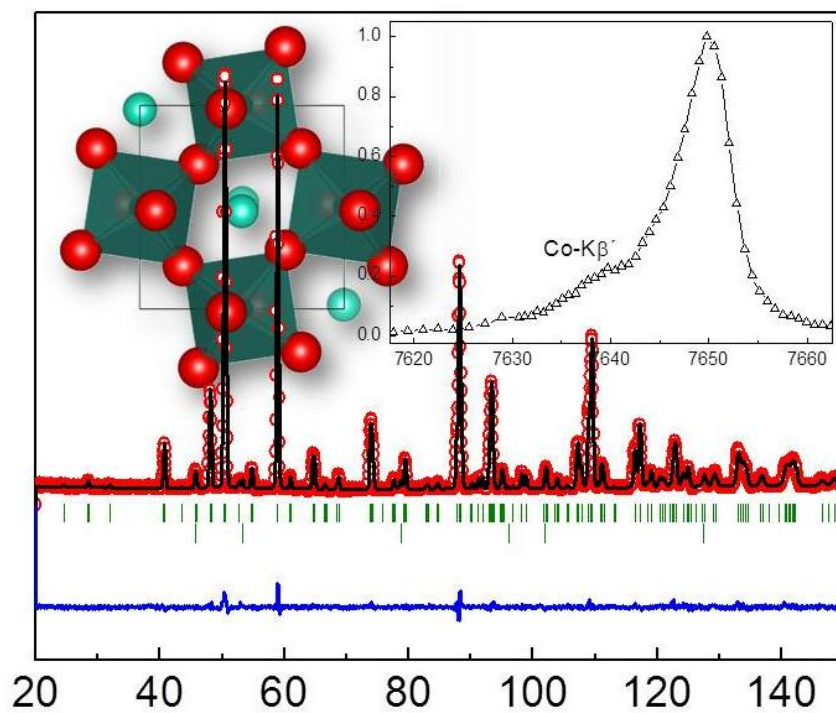
Structural information derived from the crystal structure refinement of $\text{LaCo}_{0.71(1)}\text{V}_{0.29(1)}\text{O}_{2.97(3)}$ has been deposited at the ICSD Fachinformationszentrum Karlsruhe (FIZ) (E-mail: CrysDATA@FIZ.Karlsruhe.DE), with ICSD file number 428836 (for $\text{LaCo}_{0.71(1)}\text{V}_{0.29(1)}\text{O}_{2.97(3)}$ at 300 K).

See DOI: 10.1039/b000000x/

- 1 J.A. Villoria, N. Mota, S.A. Al-Sayari, M.C. Álvarez-Galván, R.M. Navarro and J.L.G. Fierro, *Micro and Nanosystems*, 2012, **4** (3), 231.
- 2 J.B. Goodenough, *Reports on Progress in Physics*, 2004, **67** (11), 1915.
- 3 L. Ju, T. Sabergharesou, K.G. Stamplecoskie, M. Hegde, T. Wang, N.A. Combe, H. Wu and P.V. Radovanovic, *J. Am. Chem. Soc.*, 2012, **134** (2), 1136.
- 4 L. Ortega San Martín, J.P. Chapman, L. Lezama, J. Sánchez-Marcos, J. Rodríguez-Fernández, M.I. Arriortua and T. Rojo, *J. Mater. Chem.*, 2005, **15**, 183.
- 5 K. Horigane, T. Uchida, H. Hiraka, K. Yamada and J. Akimitsu, *Nuclear Instruments and Methods in Physics Research A*, 2009, **600**, 243.
- 6 M.C. Viola, M.J. Martínez-Lope, J.A. Alonso, J.L. Martínez, J.M. De Paoli, S. Pagola, J.C. Pedregosa, M.T. Fernández-Díaz and R.E. Carbonio, *Chem. Mater.*, 2003, **15**, 1655.
- 7 J.M. Chen, Y.Y. Chin, M. Valldor, Z. Hu, J.M. Lee, S.C. Haw, N. Hiraoka, H. Ishii, C.W. Pao, K.D. Tsuei, J.F. Lee, H.J. Lin, L.Y. Jang, A. Tanaka, C.T. Chen and L.H. Tjeng, *J. Am. Chem. Soc.*, 2014, **136**, 1514.

Journal Name

- 8 K.L. Holman, Q. Huang, T. Klimczuk, K. Trzebiatowski, J.W.G. Bos, E. Morosan, J.W. Lynn and R.J. Cava, *J. Solid State Chemistry*, 2007, **180**, 75.
- 9 Y. Shimakawa, S. Zhang, T. Saito, M.W. Lufaso and P.M. Woodward, *Inorg. Chem.*, 2014, **53**, 594.
- 10 T.K. Mandal, M. Croft, J. Hadermann, G. Van Tendeloo, P.W. Stephens and M. Greenblatt, *J. Mater. Chem.*, 2009, **19**, 4382.
- 11 K.I. Kobayashi, T. Kimura, H. Sawada, K. Terakura and Y. Tokura, *Nature*, 1998, **395**, 677.
- 12 S. Trasatti, *Transition metal oxides: versatile materials for electrocatalysis*, J. Lipkowski and Ph. Ross (Eds.), *Electrochemistry of Novel Materials*, 1994, **Vol. III**, VCH Publishers, 207.
- 13 W. Zhou, W. Jin, Z. Zhu and Z. Shao, *Int. J. Hydrogen Energy*, 2010, **35**, 1356.
- 14 L. Jiang, F. Li, T. Wei, R. Zeng and Y. Huang, *Electrochimica Acta*, 2014, **133**, 364.
- 15 L. Jiang, T. Wei, R. Zeng, W.X. Zhang and Y.H. Huang, *J. Power Sources*, 2013, **232**, 279.
- 16 P.G. Radaelli and S.W. Cheong, *Phys. Rev. B: Condens. Matter*, 2002, **66**, 094408.
- 17 S. Roy, M. Khan, Y.Q. Guo, J. Craig and N. Ali, *Phys. Rev. B: Condens. Matter*, 2001, **65**, 064437.
- 18 K. Ramesha, J. Gopalakrishnan, V. Smolyaninova and R.L. Greene, *J. Solid State Chemistry*, 2001, **162**, 250.
- 19 H.M. Rietveld, *J. Appl. Crystallogr.*, 1969, **2**, 65.
- 20 J. Rodriguez-Carvajal, *Physica B*, 1993, **192**, 55.
- 21 K. Momma and F. Izumi, *J. Appl. Crystallogr.*, 2011, **44**, 1272.
- 22 G. Tirao, G. Stutz and C. Cusatis, *J. Synchrotron Radiat.*, 2004, **11**, 335.
- 23 S. Ceppi, A. Mesquita, F. Pomiro, E.V. Pannunzio Miner and G. Tirao, *J. Phys. Chem. Solids*, 2014, **75**, 366.
- 24 S.D. Kelly, D. Hesterberg and B. Ravel, *Analysis of Soils and Minerals Using X-ray Absorption Spectroscopy*, in *Methods of Soil Analysis, Part 5-Mineralogical Methods*, A.L. Ulery and L.R. Drees, Eds., 2008, 367. Soil Science Society of America, Madison, WI, USA.
- 25 C.J. Howard, B.J. Kennedy and P.M. Woodward, *Acta Crystallogr. B*, 2003, **59**, 463.
- 26 P.M. Woodward, *Acta Crystallogr. B*, 1997, **53**, 32.
- 27 P. Glatzel and U. Bergmann, *Coord. Chem. Rev.*, 2005, **249**, 65.
- 28 K. Tsutsumi, H. Nakamori and K. Ichikawa, *Phys. Rev. B*, 1976, **13**, 929.
- 29 M.W. Haverkort, Z. Hu, J.C. Cezar, T. Burnus, H. Hartmann, M. Reuther, C. Zobel, T. Lorenz, A. Tanaka, N.B. Brookes, H.H. Hsieh, H.J. Lin, C.T. Chen and L.H. Tjeng, *J. Phys.: Condens. Matter*, 2006, **18**, 3.
- 30 A.M. Durand, D.P. Belanger, C.H. Booth, F. Ye, S. Chi, J.A. Fernandez-Baca and M. Bhat, *J. Phys.: Condens. Matter*, 2013, **25**, 382203.
- 31 C. Pascanut, N. Dragoe and P. Berthet, *J. Magnetism and Magnetic Materials*, 2006, **305**, 6.
- 32 Y.J. Liu, J.A. Cowen, T.A. Kaplan, D.C. DeGroot, J. Schindler, C.R. Kannewurf and M.G. Kanatzidis, *Chem. Mater.*, 1995, **7**, 1616.



Neutron powder diffraction pattern, Co-K β XES spectra and polyhedral view of orthorhombic $\text{LaCo}_{0.71}\text{V}_{0.29}\text{O}_{2.97}$ perovskite.